RSC Advances

PAPER

View Article Online
View Journal | View Issue

Cite this: *RSC Adv.*, 2020, **10**, 35917

Effects of carbon and nitrogen plasma immersion ion implantation on bioactivity of zirconia

Shuqin Guo,†[ab] Na Liu,†[c] Ke Liu,[d] Ying Li,[a] Wei Zhang,[d] Biao Zhu,[a] Bin Gu*[a] and Ning Wen*[a]

Zirconia is considered the most promising alternative material to titanium implants. However, zirconia is a biologically inert material and its surface modification is essential to obtain efficient osseointegration. Plasma immersion ion implantation (PIII) is a controllable and flexible approach that constructs functional groups on the surface of biomaterials and enhances osteogenic ability of host osteoclast cells. Zirconia disks were randomly divided into 4 groups (n = 50/group): (1) Blank, (2) C60N0, (3) C60N6, and (4) C60N18. Carbon and nitrogen plasma immersion ion implantation on zirconia (C and N_2-PIII) surface modification was completed with the corresponding parameters. When zirconia was modified by carbon and nitrogen plasma implantation, a new chemical structure was formed on the material surface while the surface roughness of the material remained unaltered. The nitrogen-containing functional groups with high potential were introduced but the bulk crystal structure of zirconia was not changed, indicating that the stability of zirconia was not affected. *In vitro* data showed that zirconia with high surface potential promoted adhesion, proliferation, and osteogenic differentiation of BMSCs. C60N6 was found to be superior to the other groups. Our results demonstrate that a zirconia surface modified by C and N_2-PIII can introduce desirable nitrogen functional groups and create a suitable extracellular environment to promote BMSCs biological activity. Taken together, these results suggest that C and N_2-PIII modified zirconia is a promising material for use in the field of medical implantation.

Received 5th July 2020
Accepted 6th September 2020

DOI: 10.1039/d0ra05853j

rsc.li/rsc-advances

Introduction

Replacement of missing teeth with implants and implant-supported prostheses are routine procedures for oral rehabilitation in partially or fully edentulous patients.[1] Osseointegration is an important factor that determines implant treatment success in artificial implant-supported prostheses.[2,3] Research on osseointegration mainly focuses on improving the process of osseointegration and on maintaining long-term stable osseointegration. Material characteristics of the implant, osteogenic differentiation of stem cells, and the microenvironment of the implant area are all important factors for good osseointegration to support the implants and increase their efficacy.

In recent years, as more patients reject metal components in the body (called the metal-free body concept), non-metallized prostheses have become the mainstream direction of oral restoration.[4] Commercial application of ceramic implants has been around for nearly 40 years.[3] The earliest implants used alumina materials but they were withdrawn from the market due to low bending strength and fracture toughness, the materials were prone to fracture when loaded unfavorably.[5] Current ceramic implants are mainly Y-TZP with good fracture toughness and flexural strength, and superior biological, aesthetic, mechanical, and optical properties.[6] In addition, recent studies have[2,7] shown that although the adsorption of blood protein, platelets and migration of osteogenic cells suggest a biological interaction with zirconia-based surfaces and yields comparable results as titanium implants in osseointegration. However, zirconia is a biologically inert material which makes it difficult for it to form an effective bond with bone tissue and the material itself is prone to aging or degradation at lower temperatures,[8] further efforts to enhance the biological and osseointegration behavior of zirconia-based implants considering chemical bonding and the deterioration of zirconia should be taken. Plasma technology is considered excellent in providing a suitable chemical microenvironment for bone marrow derived mesenchymal stem cells (BMSCs) to promote osteogenesis.[9] Plasma immersion ion implantation

[a]*Department of Stomatology, The First Medical Center, Chinese PLA General Hospital, 28 Fuxing Road, Haidian District, Beijing 100853, China. E-mail: zhubiao2015smu@126.com; gubin000@sina.com; wenningchn@163.com; liying5326@163.com; Tel: +(86) 010 66937947*

[b]*Department of Stomatology, Beijing Railway Construction Hospital, China Railway Construction Corporation, 40 Fuxing Road, Haidian District, Beijing 100855, China*

[c]*Department of Stomatology, Hainan Hospital, Chinese PLA General Hospital, Sanya, 572013, Hainan Province, China. E-mail: liuna0216@163.com*

[d]*Technical Institute of Physics and Chemistry, Chinese Academy of Sciences, Beijing 100190, China. E-mail: liuke17@mails.ucas.ac.cn; weizhang@mail.ipc.ac.cn*

† Authors contributing equally to this article.

(PIII) is a viable surface modification method which can change the surface microstructure and chemical composition of materials but does not affect the bulk properties of the materials. Studies have found that building functional groups on the surface of certain metals and polymers can improve their biological activity.[10–12] Recently, stem cell biology has emerged as basis of regenerative medicine and tissue engineering.[13] Bone marrow derived mesenchymal stem cells offer many advantages such as self-renewal and differentiation into multiple cell lineages, they can be derived from wide range of sources and are easy to isolate.[14] Many studies have reported that primary cultured BMSCs isolated from small animals such as mice, rats, or rabbits have a good biocompatibility with biomaterials.[15–17] BMSCs therapy combined with different biomaterials may improve bone regeneration in dental implantation.[18,19] Promoting osseointegration of BMSCs on the surface of zirconia ceramics was the focus of this study.

A suitable biochemical microenvironment on the surface of biomaterials has an important effect on osteogenic differentiation of stem cells. A nitrogen plasma modified surface can be used as a powerful microenvironment to regulate osteogenic differentiation of osteoblasts.[20–22] Our previous work has revealed that plasma-generated nitrogen functionalities can promote the osteoinductivity of polymers.[23] Therefore, we introduced nitrogen-containing functional groups on the surface of zirconium ceramics to create osteo-inductive microenvironment. However, compared with polymer materials,[23] zirconia ceramic materials do not have a carbon chain skeleton and fail to form functional groups that increase surface potential when directly immersed in nitrogen. Therefore, we soaked carbon by plasma implantation technology to construct an *in situ* carbonized layer and then immersed nitrogen to form a chemical structure with carbon which increased the surface potential of the materials and promoted the biological activity of the material surface.

Despite researchers have devoted significant efforts to modify zirconia regarding morphological and bioactive aspects, to enhance the biological and osseointegration behavior of zirconia-based implants, there is still no consensus on the ideal modification method, and any kind of surface modification may have an adverse effect on the strength of zirconia. In this study, on the basis of the previous research of polymer materials, we try to investigate the effects of carbon and nitrogen plasma immersion implantation on physicochemical properties and biological activity of zirconia materials.

Materials and methods

Sample preparation

A total of 200 biomedical grade zirconia disk samples (DOCERAM, Germany) with dimensions of 15 mm and a thickness of 1.8 mm were prepared. Prior to surface treatment, all samples were ground and polished with 600-, 800-, 1000-, and 1200-purpose water sandpaper and silicon carbide to achieve a smooth surface finish. Then, it was ultrasonically washed with 95% ethanol and deionized water in an ultrasonic water bath for 20 minutes and air dried. According to the different treatment parameters that are presented in Table 1, zirconia disks were placed into the plasma immersion ion implanter (multi-function ion implantation enhanced deposition equipment, Chengdu Tongchuang Material Surface Co. Ltd, China), C was implanted onto the zirconia surface under the condition of working vacuum of 2×10^{-3} Pa, the accelerating voltage was controlled to 40 kV, the current was 3 mA, and the immersion time was 60 min, nitrogen entered the vacuum chamber at the flow rate of 35 sccm (standard cubic centimeter), the working vacuum was 1×10^{-2} Pa, the acceleration voltage was 40 kV, and the current was 2 mA. The immersion amount of nitrogen element was changed by adjusting the immersion time of nitrogen plasma. Keeping the working chamber pressure to constant for 10 minutes after each step of ion implantation. Afterwards, the treated samples were taken out. Then, all samples were sterilized with 75% ethanol for 30 min, rinsed with PBS for 3 times, dried at room temperature, packaged in a sterilization bag, and stored at room temperature for later use.

Surface roughness and relative surface potential

Two-dimensional morphology of the samples was observed using a scanning electron microscope (SEM, HITACHI S-4800, HITACHI, Japan) at 1000×, 3000× and 5000× magnification. The three-dimensional shape was assessed by atomic force microscopy (AFM, Bruker Multimode 8, VECO, USA), with a scanning range of 5 μm × 5 μm. Data were processed with a NanoScope v1.40 Analysis software that obtained three-dimensional images and roughness average parameters (R_a). Relative surface potential was measured by a Kelvin probe force

Table 1 The treatment parameters of different groups[a]

Group	Step	Dose (ion per cm^2)	Plasma	Accelerating voltage/current	Injection time (min)	Working vacuum (Pa)
Blank	—	—	—	—	—	—
C60N0	a	4×10^{16}	C	40 kV/3–3.5 mA	60	2×10^{-3}
C60N6	a	4×10^{16}	C	40 kV/3–3.5 mA	60	2×10^{-3}
	b	0.667×10^{16}	N_2	40 kV/2 mA	6	1×10^{-2}
C60N18	a	4×10^{16}	C	40 kV/3–3.5 mA	60	2×10^{-3}
	b	2×10^{16}	N_2	40 kV/2 mA	18	1×10^{-2}

[a] a, the introduction of carbon was carried out; b, the immersion of nitrogen plasma.

microscope-amplitude (KPFM-AM) through a tapping mode on a Multi75E-G (budget sensor) probe. All data were measured in triplicates.

Crystallinity

The crystal phase structure of the modified sample surfaces was observed by X-ray diffraction analyzer (XRD, D8 focus, Bruker, Germany). The diffraction pattern was analyzed by software jade6 and the crystal structure was determined.

Chemical structure

The elemental chemical composition and chemical structure of samples were detected by X-ray photoelectron spectroscopy (XPS; ESCALAB 250Xi, ThermoFisher Scientific, UK). Data were collected and analyzed by using the Multipak software.

Bone marrow-derived mesenchymal stem cell culture

BMSCs were derived from 4 week-old Sprague Dawley rats (Charles River Co, Ltd, China). Rats were sacrificed by cervical dislocation and soaked in 75% ethanol for 30 min and the femoral bone marrow cavity was exposed under aseptic conditions. The bone marrow cavity was washed with Alpha Modified Eagle's medium (α-MEM, Gibco, USA) containing 10% fetal bovine serum (Gibco, USA), and was resuspended into a single cell suspension. Cells were cultured in a humidified air incubator at 37 °C with 5% CO_2. To obtain homogeneous population of BMSCs, single-cell-derived colony cultures were generated by a limiting-dilution technique[24] and only cells in passages 3–5 were used for further experiment. BMSCs were inoculated on zirconia disks at a density of 5×10^4 cells per cm^2 in 24-well plates (Corning, USA). Culture medium was replaced every three days. All animal experiments were approved by ethics committees Committee of Ethics in Research of Medical School of Chinese PLA (2019022393).

Phenotype identification of BMSCs

To identify connatural characteristics of stem cells harvested from rat bone marrow, single-cell suspension generated from BMSCs from passage 3 were used. BMSCs were incubated with fluorescent labeled antibodies for CD44, CD45, CD31, CD34, CD73, CD90, CD105 and CD29 markers (BD, Biosciences, USA), at 4 °C in dark for 30 min. Then, cells were washed with PBS buffer and subjected to flow cytometric analysis using a CytoFLEX flow cytometry (Beckman Coulter, USA).

Cell morphology and attachment

Cells were seeded on zirconia disks for 24 h following which the culture medium was removed and samples were rinsed with sterile PBS three times. Cells absorbed on samples were fixed with 4% (v/v) paraformaldehyde (Sigma, USA) for 30 min at 4 °C. Cells were then permeabilized with 0.5% Triton X-100 at room temperature for 10 min. Samples were stained with 6-YF488-P12-phalloidin (US Everbright Inc, China) at room temperature for 1 h and with 4,6-diamidino-2-phenylindole (DAPI, Roche, Switzerland) at room temperature for 15 min. After staining, samples were rinsed three times with PBS. Finally, cell morphology was observed by inverted fluorescence microscope (AR-siMP-LSM-Kit-Legend Elite-USX, Nikon, Japan).

Cells adhered on zirconia disks were fixed with 4% paraformaldehyde (Sigma, USA) and 2.5% glutaraldehyde solution at a ratio of 1 : 1 for 30 min at 4 °C. Samples were washed three times with PBS, and dehydrated with 30%, 50%, 75%, 90%, 100% (v/v) grade ethanol for 15 min each. Samples were dried in a vacuum dryer at the critical point of CO_2, and a gold layer was sprayed. A total of 24 samples (n = 3/group) were used to observe disk-adherent cells.

Cell proliferation assay

After incubation of cells on treated or control zirconia disks for 1, 3, 5 and 7 days, the medium was removed from the plates and the disks were rinsed with sterile PBS three times and transferred into new 24-well plates. Then, 40 μL Cell Count Kit-8 (Solarbio, Beijing, China) solution and 360 μL medium were thoroughly mixed and placed into a new culture plate. After incubation for 2 h at 37 °C, 100 μL of the medium was transferred to a 96-well plate for measurement, in triplicates. Absorbance at 450 nm was measured with a microplate reader (iMark, Bio-Rad, USA).Values represent the mean ± SD of 3 independent experiments.

Alkaline phosphatase activity assay

Alkaline phosphatase (ALP) activity was measured after culturing the BMSCs on the disks for 7 and 14 days. Samples were rinsed with PBS three times and fixed in 4% paraformaldehyde solution for 15 minutes. Fixed cells were stained using an ALP chromogenic kit (Beyotime Biotechnology, Shanghai, China) at room temperature for 30 minutes. ALP activity of BMSCs grown on zirconia disks surface was detected using ALP Assay Kit (Beyotime Biotechnology, Shanghai, China). A total of 24 samples (n = 3/group) were used. After

Table 2 Primers used for real-time qPCR

Gene	Forward	Reverse
Runx2	ACTTCCTGTGCTCGGTGCT	GACGGTTATGGTCAAGGTGAA
COL I	GCCTCCCAGAACATCACCTA	GCAGGGACTTCTTGAGGTTG
OCN	AAGCAGGAGGGCAATAAGGT	CCGTAGATGCGTTTGTAGGC
OPN	AGACCATGCAGAGAGCGAG	ACGTCTGCTTGTGTGCTGG
β-Actin	GGGTCCTCTGTGAACTTGCTC	TGTAATCCTGTGGCTTGTCCTC

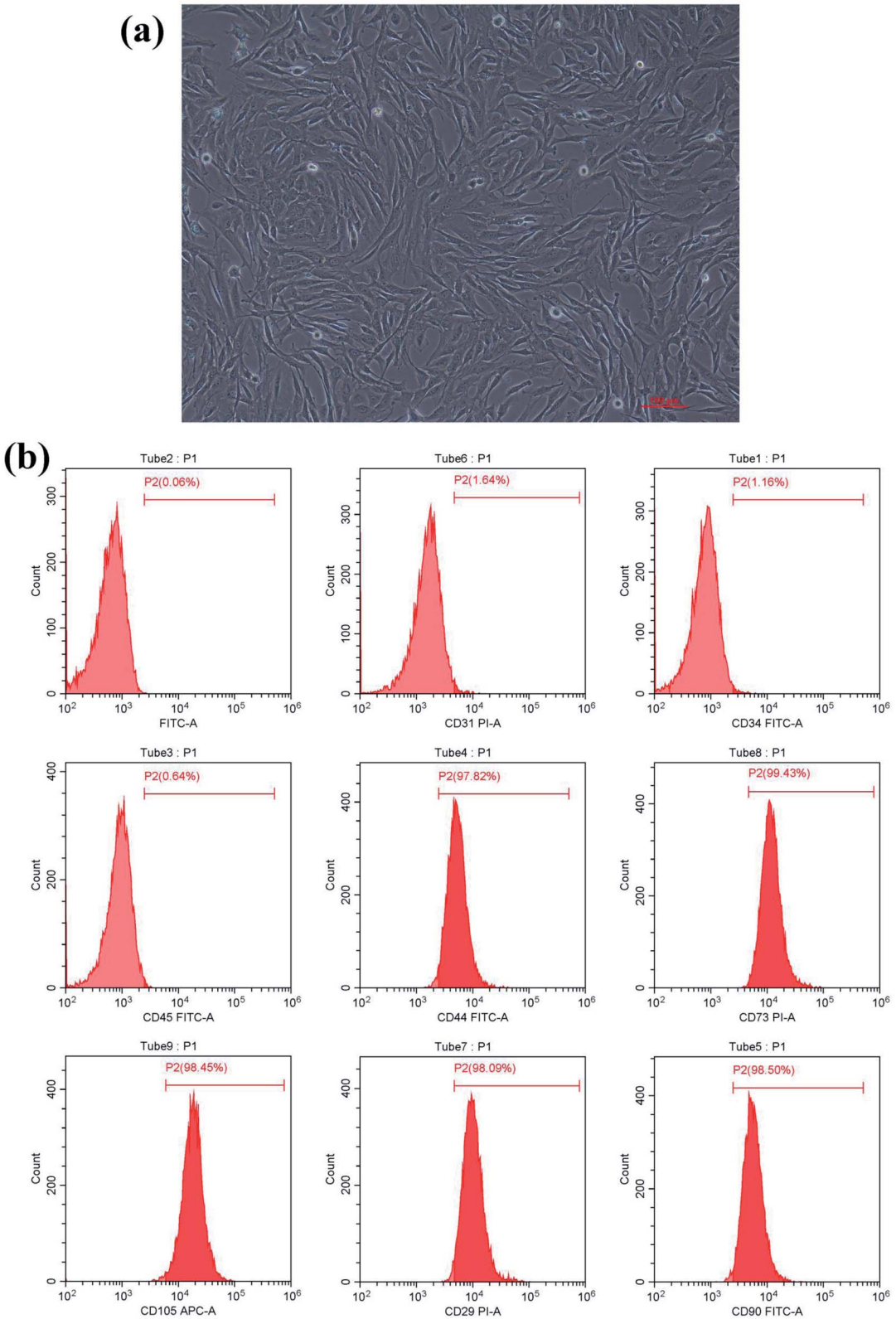

Fig. 1 Morphological characteristics of BMSCs. (a) BMSC morphology as observed by inverted aberration microscope, scale = 100 μm. (b) BMSCs highly expressed mesenchymal stem cell surface antigens: CD44 (97.82%), CD73 (99.43%), CD105 (98.45%), CD29 (98.09%) and CD90 (98.40%), lacked expression of hematopoietic stem cell surface markers CD31 (1.64%), CD34 (1.16%), and CD45 (0.64%).

culturing the cells for 7 and 14 days, samples were rinsed with PBS two times and immersed in cell lysis buffer (Beyotime Biotechnology, Shanghai, China) for 1 min. The lysate was centrifuged 12 000 rpm for 5 min, and the supernatant was collected. Absorbance value was measured at 405 nm wavelength with a microplate reader. Alkaline phosphatase activity was calculated according to the manufacturer's protocol.

Extracellular matrix mineralization

When the cells grown on zirconia disks reached 60–70% confluency, culturing medium was substituted with osteogenic induction medium (BMSC culturing medium supplemented with 10^{-8} M dexamethasone, 10 mM β-glycerophosphate, and 50 μg mL^{-1} ascorbic acid) which was replaced every three days. After culturing the cells for 21 days, the medium was aspirated and samples were rinsed with PBS 3 times. Samples were fixed with 4% paraformaldehyde solution for 15 minutes and stained with alizarin red S staining solution (Cyagen, USA) for 30 minutes at 37 °C. Samples were observed and photographed under an upright optical microscope (Ni-U, Nikon, Japan). Staining was quantified by adding 10% cetylpyridinium chloride for 1 hour at room temperature to extract alizarin red S–calcium complex. Finally, 100 μL of the solution was added to a 96-well plate and absorbance at 562 nm was measured with a microplate reader (3 disks for each zirconia surface).

Quantitative real time-polymerase chain reaction (q-PCR)

Cells were harvested at 7 d and 14 d after osteoblast differentiation and total RNA was extracted by Trizol reagent (Invitrogen). RNA was reverse-transcribed into cDNA with Super Script First Stand Strand Synthesis kit (Invitrogen) using manufacturer's protocol. qPCR was performed using TransScript II Green One-Step q-PCR SuperMix kit (Toyobo, Osaka, Japan) on BioRad-7500 qPCR system. The reaction mix for qPCR was 20 μL which included 0.5 μL forward and 0.5 μL reverse primer, 10 μL 2× supermix, 7 μL ddH_2O and 2 μL cDNA. The reaction conditions were as follows: denaturation at 95 °C for 3 min, 95 °C for 30 s, 60 °C for 1 min, 40 cycles. Data was recorded by BioRad-7500 real-time PCR instrument and the final results were calculated by the software based on the standard curve. This experiment was performed in triplicates. The following rat primers were listed in Table 2.

Statistical analysis

Statistical analyses were conducted using SPSS 22.0 software (Chicago, IL, USA). All measurements were independently performed at least three times. Values were reported as mean ± standard deviation. Statistical significance was analyzed by one-way ANOVA following with Bonferroni *post hoc* tests when equal variances were assumed or Tamhane's T2 *post hoc* tests when equal variances were not assumed for comparisons between two

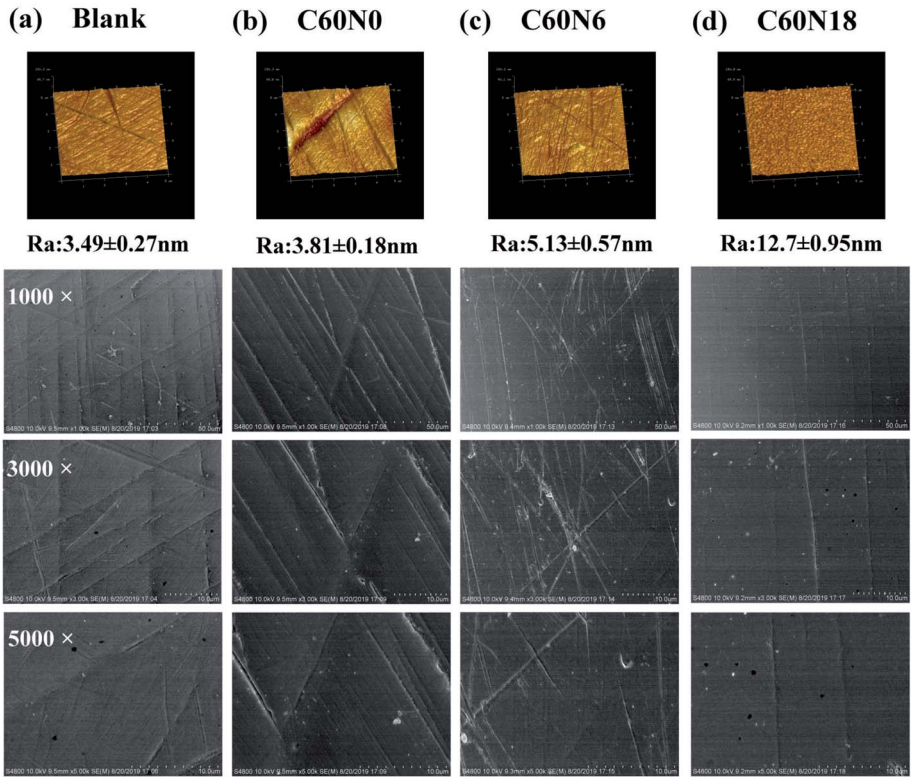

Fig. 2 Atomic force microscopy (AFM) images showing three-dimensional morphologies and the roughness (R_a) of the material surfaces. (a) Blank, (b) C60N0, (c) C60N6, (d) C60N18. Scanning electron microscopy (SEM) of two-dimensional morphological surfaces. Images are magnified 1000×, 3000×, and 5000×.

or multiple groups. Homogeneity of variance was tested using Levene's test, $P < 0.05$ was considered significant.

Results

BMSCs displayed connatural characteristics of stem cells

After culturing for 3 days, the isolated BMSCs were found adhering to the wall of the plate and appeared like colonies with irregular morphology. After 7 days, the number of adherent cells increased significantly. After 10 days of culturing, cells reached 90% confluency. After passage, cells appeared in the shape of long strips or spindles (Fig. 1a) and grew rapidly, reaching 90% confluency in about a week. Phenotype identification (Fig. 1b) showed that BMSCs highly expressed mesenchymal stem cell surface antigens: CD44 (97.82%), CD73 (99.43%), CD105 (98.45%), CD29 (98.09%) and CD90 (98.40%). Cells lacked expression of hematopoietic stem cell surface markers CD31 (1.64%), CD34 (1.16%), and CD45 (0.64%). Taken together, these results suggest that mesenchymal stem cells were isolated and cultured successfully.

Surface morphology characterization of zirconia samples

SEM showed the surface of C60N0, C60N6, C60N18 showed small amounts of irregular fine lines when compared to the blank surface group which was relatively flat (Fig. 2a–d, bottom panel). AFM showed that blank surface was relatively smooth with a R_a of 3.49 ± 0.27 nm (Fig. 2a, upper panel). The R_a values of C60N0, C60N6, C60N18 were 3.81 ± 0.18 nm, 5.13 ± 0.57 nm, and 12.70 ± 0.95 nm, respectively (Fig. 2b–d, upper panel). SEM evaluation and quantitative assessment of the topographic

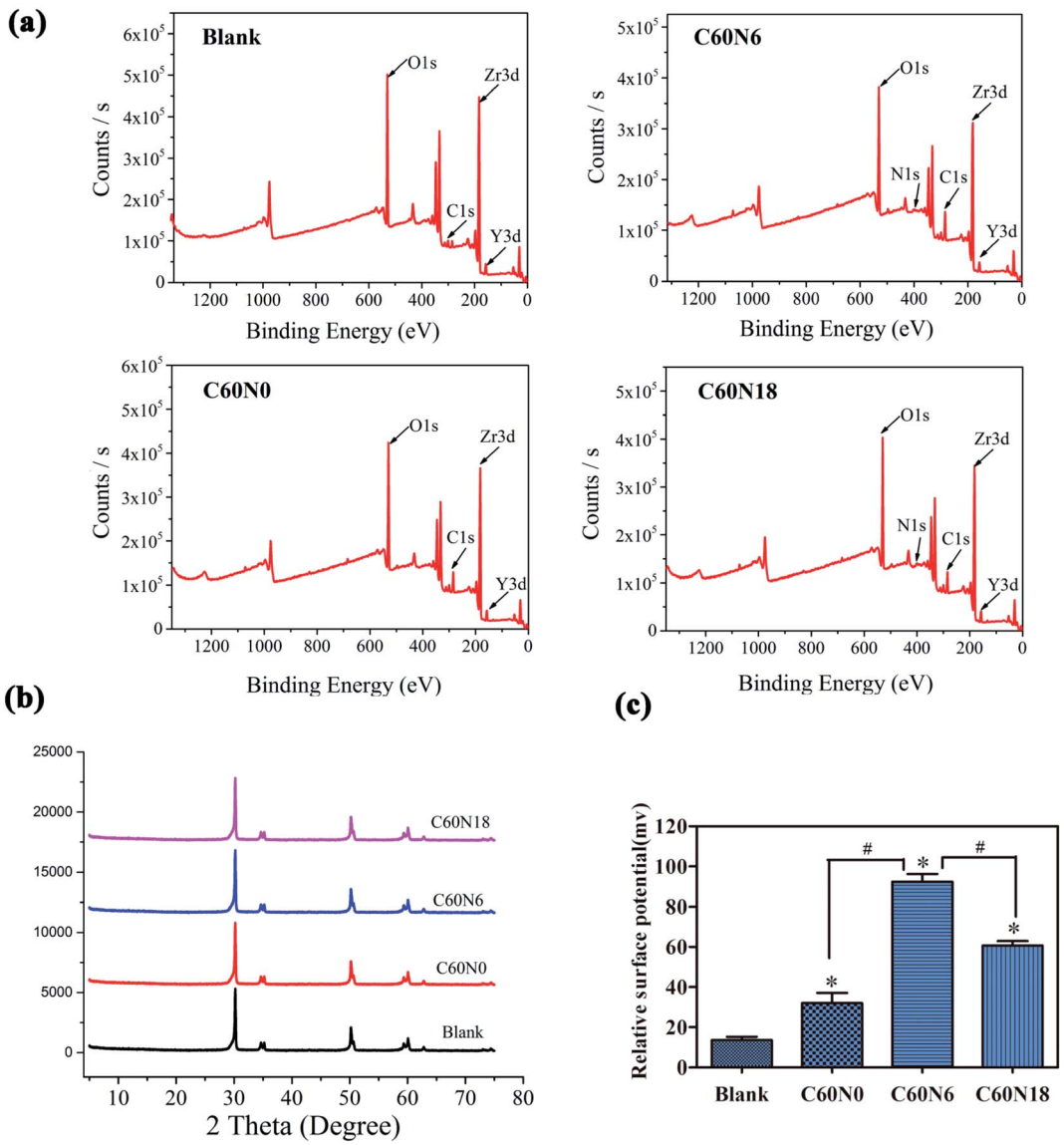

Fig. 3 Surface analysis of C and N_2 plasma treated materials. (a) X-ray photoelectron spectroscopy (XPS) full spectra of blank, C60N0, C60N6, and C60N18. (b) X-ray diffraction (XRD) patterns of different zirconia disks. (c) Relative surface potential of blank, C60N0, C60N6, and C60N18 (*, $P < 0.05$ compared with blank; #, $P < 0.05$ compared with C60N0, C60N18).

Table 3 Chemical composition of different samples measured using XPS

Group	Zr	O	C	Y	N
Blank	27.06	61.17	7.98	2.38	1.42
C60N0	21.65	50.79	24.59	1.65	1.32
C60N6	17.74	51.9	26.13	1.53	1.97
C60N18	20.12	52.2	23.17	1.75	2.76

configuration by AFM demonstrated that C and N_2 plasma treatment did not alter surface morphology characteristics of different zirconia samples, there was no significant difference between the sample groups.

Surface chemical structure and relative potential by C and N_2 plasma treatment

XPS results showed binding energy of elements to form chemical bonds and chemical composition of different modified samples. XPS analysis demonstrated that the carbon and nitrogen content on the surface of modified zirconia increased. Compared to blank, the surface element ratios of the other three zirconia sample groups changed significantly after plasma treatment (Fig. 3a). The C and N element composition ratio of blank surface was 7.98% and 1.42% respectively, while the C and N element composition ratio increased to 24.59% and 1.32% in C60N0, 26.13% and 1.97% in C60N6, and 23.17% and 2.76% in C60N18, respectively (Table 3). This data confirmed that the C and N elements were successfully implanted onto the surface of plasma-treated zirconia materials. XRD analysis also revealed the surface crystal structure of blank, C60N0, C60N6, and C60N18. The peak at 30.5° showed tetragonal zirconia which was the main body of yttrium-stabilized zirconia and the crystal composition of the test piece conformed to yttrium-stabilized zirconia (Fig. 3b). Compared with the control group, the crystal phase results of the modified samples treated with C and N_2-PIII did not change significantly and no obvious monoclinic phase was observed. However, the surface potential of zirconia disks in the plasma treatment group was significantly improved when compared to the control group. Moreover, the surface potential of the C60N6 group was higher than the other two groups (Fig. 3c). This confirmed that after plasma

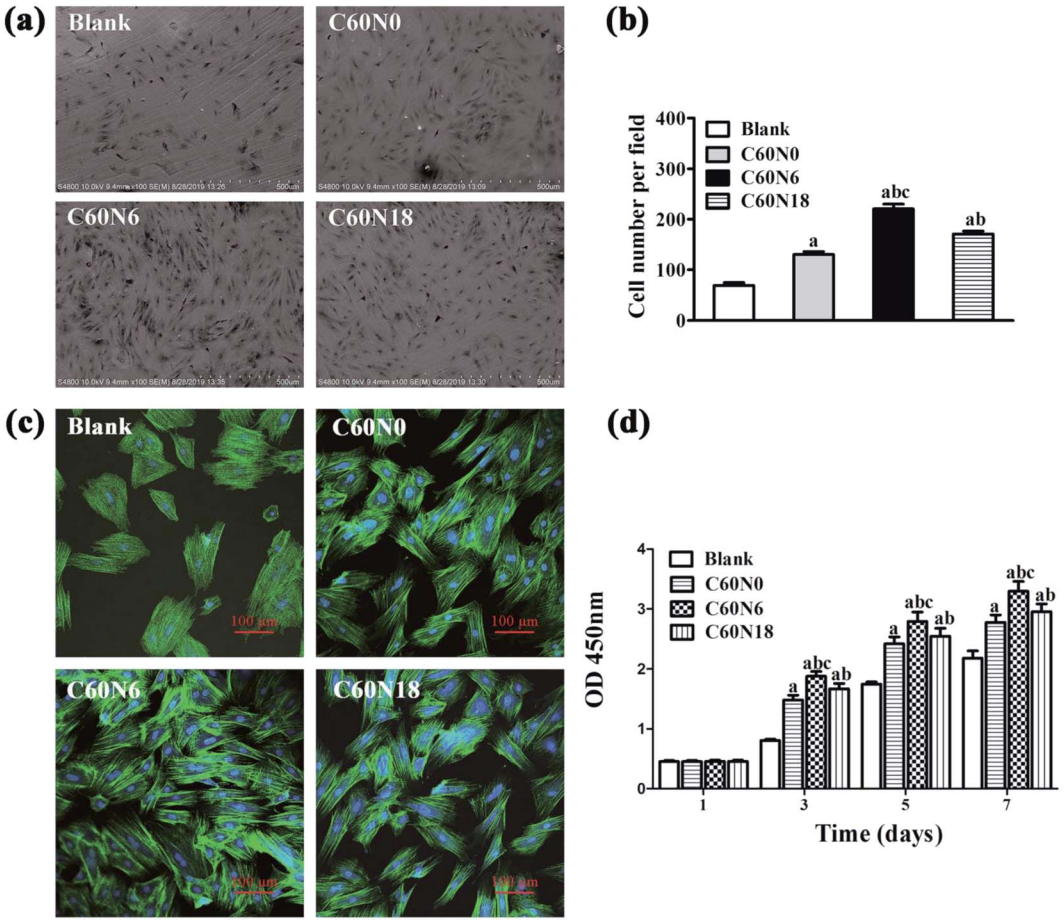

Fig. 4 Cell morphology and cell attachment of cultures grown on zirconia surfaces at 24 h. (a) Cells adhesion on the surface of different zirconia disks as observed by SEM. (b) The number of cells adhered to surface of different samples was analyzed by Image J software. (c) Fluorescence microscopy images of cells stained with DAPI for nuclei (blue) and phalloidin for actin filaments (green). (d) Cell proliferation on the surface of different samples as performed by CCK-8 kit. a, $P < 0.05$ compared with Blank; b, $P < 0.05$ compared with C60N0; c, $P < 0.05$ compared with C60N18.

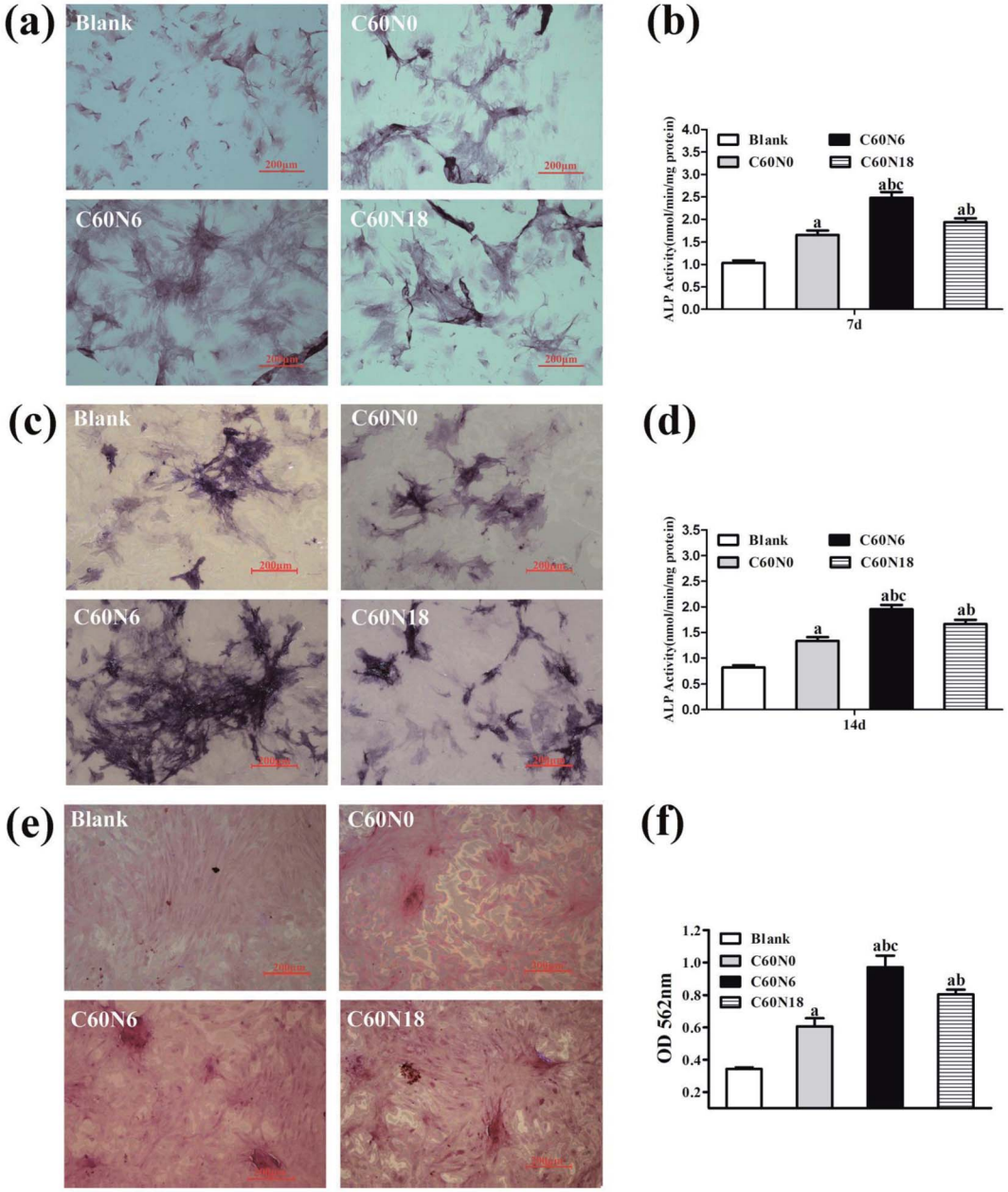

Fig. 5 Osteoblast differentiation potential of cells on the surface of modified zirconia materials. (a) Alkaline phosphatase (ALP) staining of cultured cells on different samples at 7 d. (b) ALP activity of cells cultured on zirconia disk surfaces after 7 days. (c) ALP staining of cultured cells on different samples at 14 d. (d) ALP activity of cells cultured on zirconia disk surfaces after 14 days. (e) Extracellular matrix mineralization at day 21 of cultures grown on zirconia surfaces. (f) The amount of mineralized extracellular matrix on zirconia disks. Data are shown as the mean ± SD; a, $P < 0.05$ compared with blank; b, $P < 0.05$ compared with C60N0; c, $P < 0.05$ compared with C60N18.

treatment, the corresponding functional groups were introduced on the surface of the materials thereby increasing the surface potential of the materials.

Effects of plasma insertion of nitrogen functionalities on proliferation and adhesion of BMSC

We examined cell adhesion and morphology after seeding BMSCs on zirconia disks for 24 h, by SEM (Fig. 4a). Compared to the untreated blank surface, cells that were attached to the modified samples were arranged more closely. Also, the number of cells on modified samples surface was significantly higher ($P < 0.05$). The amount of cells attached on C60N6 surface was highest among the four groups ($P < 0.05$) (Fig. 4b). Fluorescence microscopy images revealed that cells on the surface of blank were slightly stretched and hemispherical and showed a small amount of filopodia. After treatment with C and N_2-PIII, cells on the surface of C60N0, C60N6, and C60N18 extended fully with more pseudopodia. Cells on the surface of C60N6 were most pronounced particularly, with more intercellular connections

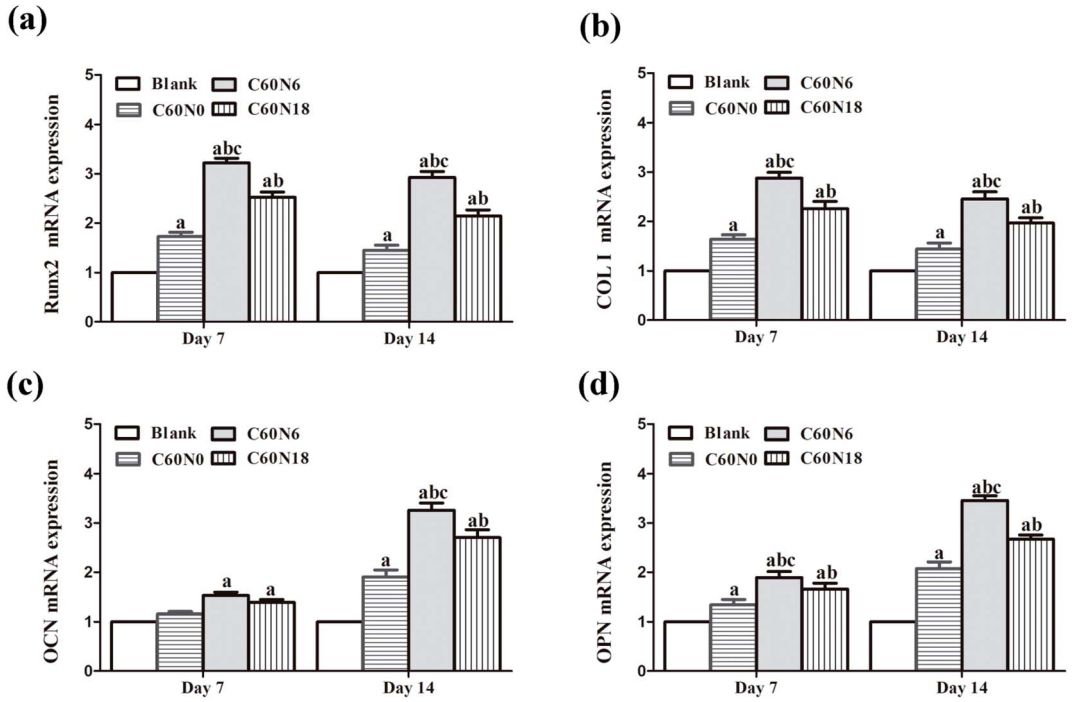

Fig. 6 Expression of osteogenesis related genes. mRNA expression of (a) Runx2, (b) Col I, (c) OCN, and (d) OPN in cells cultured on different samples for 7 and 14 days. a, $P < 0.05$ compared with blank; b, $P < 0.05$ compared with C60N0; c, $P < 0.05$ compared with C60N18.

tightly attached to the surface of the material demonstrating better cell compatibility (Fig. 4c).

Cell proliferation on zirconia disks was analyzed by CCK-8 assay at 1 d, 3 d, 5 d and 7 d of culturing (Fig. 4d). Results show that after 1 day, there was no significant difference in cell absorbance among different groups. After 3, 5 and 7 days, the cell absorbance values of zirconia materials modified by carbon and nitrogen plasma were significantly higher than those of the control group ($P < 0.05$), and C60N6 group showed the highest absorbance among all the groups. The results indicated zirconia treated by C and N_2-PIII promoted cell proliferation activity.

Osteoblast differentiation potential of cells on the surface of modified zirconia materials

BMSCs were harvested after 7, 14 and 21 days of culturing on zirconia surfaces and osteoblast differentiation potential was investigated by measuring ALP staining. After 7 days, the cell membrane and cytoplasmic granules on the surface of the modified zirconia materials were positive when compared to the blank control (Fig. 5a). At day 14, the cell staining positive reaction was more obvious with blue-black particles and block-like deep-dyed particles (Fig. 5c). We also performed ALP activity assay at 7 d and 14 d to verify the effect of C and N_2-PIII on differentiation of BMSCs. Results (Fig. 5b) showed that the alkaline phosphatase activity of cultured cells on the plasma modified surfaces at day 7 was significantly higher than that on untreated surfaces, and C60N6 group was superior to other groups ($P < 0.05$). The ALP activity after 14 days culture period was similar to day 7 results (Fig. 5d). After 21 days, cells grown on plasma treated surfaces overlapped and formed mineralized nodes with a large amount of mineral deposits in the interstitial space which showed red color. The untreated surfaces had no obvious mineralized nodules formation (Fig. 5e). Semi-quantitative results (Fig. 5f) presented that the OD value of plasma treated groups was higher than that of untreated group, and C60N6 group was highest ($P < 0.05$).

Expression of osteogenesis related genes

We evaluated mRNA expressions of the bone marker genes Runx2, Col I, OCN and OPN after BMSCs were cultured on samples for 7 and 14 days. Data analyzed from qPCR showed that the expression of osteogenesis related genes was significantly increased in cells cultured on C and N_2-PIII treated samples. Compared to other groups at day 7 and day 14, the expression level of C60N6 was significantly higher ($P < 0.05$). Among all the different groups, the expression levels of Runx2 (Fig. 6a) and Col I (Fig. 6b) were the highest at 7 d and decreased slightly at 14 d while the expression levels of OCN (Fig. 6c) and OPN (Fig. 6d) increased slightly at 7 d and increased significantly at 14 d.

Discussion

Zirconia is an all-ceramic material with good biocompatibility, stable mechanical properties, and good aesthetics. Application of oral fixed denture restoration and dental implant has been widely studied and it has a broad application prospect in the field of implant surgery. However, zirconia material has a poor biological activity and does not form effective bond with the bone tissue which limits its wide clinical application.[4,25,26]

Plasma is an aggregation state with high energy of matter and is the most important state of matter in the universe. Plasma research has developed rapidly in recent years and has extended to the fields of biomedicine, environment, aerospace, agriculture, and military.[27] PIII technology is a new surface modification technology based on traditional plasma techniques which can not only improve the surface activity of biomaterial but also retains its bulk properties. It has been widely used in the surface modification of polymers and metals.[18,19,28,29]

In this study, we implanted carbon on the surface of zirconia materials by plasma immersion technology to construct an *in situ* carbonized layer. We then injected nitrogen to form a chemical structure with carbon forming a non-polar covalent bond on the surface of the materials which slightly increased the surface potential. Nitrogen plasma is usually composed of various nitrogen groups such as N_2, N_2 (excited) and N. Nitrogen functionalities with the structures of C–N, C═N, N–O, N═C–O and N–C═O were formed on the surface of zirconia materials.[30,31] With the immersion of nitrogen, a tertiary amine-like structure of C–N(C)–C group was further formed on the surface of C60N6 group and C60N18 group, a polar group with positive charge which increased the surface potential. This structure was analyzed on polymer materials in our previous study.[23] In this study, XPS energy spectrum analysis showed that C and N elements were implanted on the surface of zirconia ceramics treated by C and N_2 plasma resulting in an increase in the percentage content of C and N elements. The results indicated that the new chemical structures were formed on the surface of plasma treated zirconia materials and the nitrogen-containing functional structures were introduced into the surface of the samples.

Any surface modification method should take into account the phase transformation of zirconia. When external force is applied to the tetragonal zirconia, it may lead to local microfracture of the material. When stress is concentrated at the fracture tip, the tetragonal phase transforms into monoclinic phase and volume expands at the same time. As the monoclinic phase zirconia increases, the surface microfracture of the material gradually increases and the surface coarsening structure occurs leading to the fracture of zirconia materials.[32] At present, zirconia implants are generally treated with surface treatments such as grinding, sandblasting, and acid etching to enhance osseointegration. These surface treatment methods may lead to phase transformation from tetragonal zirconia to monoclinic zirconia, as well as surface microcracks resulting in changes in mechanical properties in terms of static and fatigue strength.[7] In this study, scanning electron microscope (SEM) and atomic force microscope (AFM) showed that the plasma technology had no obvious effect on the surface morphology of zirconia materials. The X-ray diffractometer analysis further confirmed that the surface crystal phase structure of the treated zirconia samples did not change and there was no obvious monoclinic phase which confirmed that the carbon and nitrogen plasma immersion implantation technology did not destroy the bulk structure of zirconia material and had no detrimental effect on its stability.

Studies have shown that nitrogen-containing groups prepared by plasma technology show good cytocompatibility and can even promote osteogenic differentiation of osteocytes.[33–35] In our previous studies,[23,31] nitrogen-containing groups were introduced on the surface of polymer materials by plasma technology which inhibited bacterial growth but promoted the growth of osteocytes, it was further found that the nitrogen-containing functional groups on the surface increased surface potential and endowed the surface with antibacterial and bone-inducing activity, among these, the surface rich in tertiary nitrogen group (C–N(C)2) had better antibacterial and bone-inducing activity. Gorth *et al.*[36] found that the C–N structure prepared in PEEK material had bacteriostatic ability, biocompatibility, and excellent mechanical properties. In our previous studies,[23,37] we have also shown that the nitrogen function produced by plasma can up-regulate osteogenesis of bone marrow mesenchymal stem cells. These observations confirm the feasibility to obtain high surface potential and improve the biological activity of materials by constructing nitrogen-containing functional structures.

Surface characteristics of biomaterials play an important role in the process of osseointegration. Surface properties and morphology of biomaterials may promote cell adhesion, proliferation, and osteogenic differentiation.[38,39] We evaluated biocompatibility of the materials by observing cell adhesion, proliferation, mineralization, and by measuring the expression of osteogenesis-related genes. We found that a large number of BMSCs adhered to zirconia materials treated with C and N_2-PIII, and spread more obviously after cell adhesion at the initial stage, protruding more pseudopodia. This was especially true for C60N6 group where cells on the surface of zirconia materials extended most obviously, arranged closely, and also attached to the material surface closely, showing better cytocompatibility. Surface characteristics of the materials may affect the behavior of cells indicating that surface of the material treated by plasma was more conducive to cell adhesion. We further showed that the cell proliferation activity of C60N0 group, C60N6 group and C60N18 group was higher than that of the blank group with, C60N6 group showing the highest proliferation potential. This may be due to the fact that when the nitrogen-containing functional groups were implanted on the surface of the materials after plasma treatment, a suitable microenvironment was created which promoted cell adhesion and proliferation, C60N6 group of high relative potential was more suitable for the biological behavior of cells. Previous studies[17,34,40,41] have also shown that positively charged nitrogen functionalities could promote cell expression thus improving biological activity, which was consistent with our findings.

Alkaline phosphatase (ALP) is a marker of early osteogenic differentiation and contributes to bone tissue mineralization.[42] Compared to cells on untreated zirconia materials, cells grown on the surface treated with C and N_2-PIII had a higher alkaline phosphatase activity. Mineralization of cells is an important sign of new bone formation. In order to further verify the effect of C and N_2-PIII treated zirconia on osteogenic differentiation of BMSCs, we used alizarin staining and quantitative methods to detect the mineralization ability of growing cells on different

substrates. When cells were co-cultured with the samples for 21 days, a deep red large calcium nodule formed between alizarin and calcium salt in the treated group. Cells grown on plasma treated materials had higher mineralization which once again proved that the surface nitrogen structure promoted osteogenic differentiation of BMSCs. In order to explain the molecular mechanism underlying the response of nitrogen-containing groups on the surface of zirconia materials produced by C and N_2-PIII, the expression of osteogenic-related genes such as osteocalcin (OCN), osteopontin (OPN), type I collagen (Col I) and transcription factor Runx2 in BMSCs were detected by qPCR. OCN and OPN are non-collagen matrix proteins which play an important role in bone remodeling and mineralization[43,44] and promote integration between implant and the bone tissue. Col I plays an important role in the development and balance of osteoblast phenotype.[45] Runx2, as an important bone-specific transcription factor, is an early marker of osteoblasts.[46] At 7 days and 14 days post-culture, BMSCs grown on C and N_2-PIII treated samples had higher expression of Runx2, Col I, OCN, and OPN than cells grown on untreated zirconia disk with, the expression being more obvious in the C60N6 group. It is worth noting that in each group, the expression levels of Runx2 and Col I were higher on day 7 and decreased slightly on day 14 because Runx2 and Col I are markers of early differentiation. With the extension of time, expression of OCN and OPN increased significantly on day 14 indicating that plasma-treated zirconia materials enhanced the effect of late osteogenic differentiation. In conclusion, within the limits of this investigation, zirconia surface modified by C and N_2-PIII can introduce desirable nitrogen functionalities and create a suitable extracellular environment to promote BMSCs biological activity. In addition, the PIII technology did not alter the crystal structure and morphology of zirconia ceramic surface suggesting that the surface mechanical properties were not affected. However, further studies, such as *in vivo* investigations are necessary to prove the reliability of the method for the surface modification of dental implants of zirconia. Furthermore, the mechanism regarding the effects of C and N_2-PIII on bioactivity of zirconia was not clearly defined. Therefore, more studies are needed.

Conclusions

In this study, when zirconia surface modified by carbon and nitrogen plasma immersion ion implantation, a new chemical structure was formed on the material surface while the surface roughness of the material remained unaltered. The nitrogen-containing functional groups with high potential were introduced but the bulk crystal structure of zirconia was not changed indicating that the stability of zirconia was not affected. Desirable nitrogen functionalities created a suitable extracellular environment to promote the adhesion, proliferation and osteogenic differentiation of BMSCs, C60N6 was found to be superior to the other groups. Our experiment lays the foundation for providing new strategies for extensive development of zirconia materials in the field of medical implantation.

Conflicts of interest

There are no conflicts to declare.

Acknowledgements

This study was supported by National Natural Science Foundation of China (NFSC 51972339, NFSC 51802350) and project funded by Scientific and Technological Innovation Nursery Fund Project of PLA General Hospital (18KMM13) and China Postdoctoral Science Foundation (2019T120980).

References

1 D. D. Bosshardt, V. Chappuis and D. Buser, Osseointegration of titanium, titanium alloy and zirconia dental implants: current knowledge and open questions, *Periodontol. 2000*, 2017, **73**, 22–40.
2 G. Manzano, L. R. Herrero and J. Montero, Comparison of clinical performance of zirconia implants and titanium implants in animal models: a systematic review, *Int. J. Oral Maxillofac. Implants*, 2014, **29**, 311–320.
3 S. Pieralli, R. J. Kohal, E. Lopez Hernandez, S. Doerken and B. C. Spies, Osseointegration of zirconia dental implants in animal investigations: A systematic review and meta-analysis, *Dent. Mater.*, 2018, **34**, 171–182.
4 H. Nishihara, M. Haro Adanez and W. Att, Current status of zirconia implants in dentistry: preclinical tests, *J. Prosthodont. Res.*, 2019, **63**, 1–14.
5 M. Andreiotelli, H. J. Wenz and R. J. Kohal, Are ceramic implants a viable alternative to titanium implants? A systematic literature review, *Clin. Oral Implants Res.*, 2009, **20**(suppl. 4), 32–47.
6 K. Sivaraman, A. Chopra, A. I. Narayan and D. Balakrishnan, Is zirconia a viable alternative to titanium for oral implant? A critical review, *J. Prosthodont. Res.*, 2018, **62**, 121–133.
7 F. H. Schünemann, M. E. Galárraga-Vinueza, R. Magini, M. Fredel, F. Silva, J. C. M. Souza, Y. Zhang and B. Henriques, Zirconia surface modifications for implant dentistry, *Mater. Sci. Eng., C*, 2019, **98**, 1294–1305.
8 N. Cionca, D. Hashim and A. Mombelli, Zirconia dental implants: where are we now, and where are we heading?, *Periodontol. 2000*, 2017, **73**, 241–258.
9 W. Zhang, J. Liu, H. Shi, N. Liu, K. Yang, L. Shi, B. Gu, H. Wang, J. Ji and P. K. Chu, Effects of plasma-generated nitrogen functionalities on the upregulation of osteogenesis of bone marrow-derived mesenchymal stem cells, *J. Mater. Chem. B*, 2015, **3**, 1856–1863.
10 Y. Zhao, S. M. Wong, H. M. Wong, S. Wu, T. Hu, K. W. Yeung and P. K. Chu, Effects of carbon and nitrogen plasma immersion ion implantation on in vitro and in vivo biocompatibility of titanium alloy, *ACS Appl. Mater. Interfaces*, 2013, **5**, 1510–1516.
11 E. A. Wakelin, A. Fathi, M. Kracica, G. C. Yeo, S. G. Wise, A. S. Weiss, D. G. McCulloch, F. Dehghani, D. R. McKenzie and M. M. Bilek, Mechanical Properties of Plasma Immersion Ion Implanted PEEK for Bioactivation of

Medical Devices, *ACS Appl. Mater. Interfaces*, 2015, **7**, 23029–23040.

12 M. Chen, L. Ouyang, T. Lu, H. Wang, F. Meng, Y. Yang, C. Ning, J. Ma and X. Liu, Enhanced Bioactivity and Bacteriostasis of Surface Fluorinated Polyetheretherketone, *ACS Appl. Mater. Interfaces*, 2017, **9**, 16824–16833.

13 S. Razzouk and R. Schoor, Mesenchymal stem cells and their challenges for bone regeneration and osseointegration, *J. Periodontol.*, 2012, **83**, 547–550.

14 C. L. Tsai, P. C. Wu, M. E. Fini and S. Shi, Identification of multipotent stem/progenitor cells in murine sclera, *Invest. Ophthalmol. Visual Sci.*, 2011, **52**, 5481–5487.

15 P. Capellato, A. L. Escada, K. C. Popat and A. P. Claro, Interaction between mesenchymal stem cells and Ti-30Ta alloy after surface treatment, *J. Biomed. Mater. Res., Part A*, 2014, **102**, 2147–2156.

16 S. Strauss, A. Neumeister, S. Barcikowski, D. Kracht, J. W. Kuhbier, C. Radtke, K. Reimers and P. M. Vogt, Adhesion, vitality and osteogenic differentiation capacity of adipose derived stem cells seeded on nitinol nanoparticle coatings, *PLoS One*, 2013, **8**, e53309.

17 J. Veevers-Lowe, S. G. Ball, A. Shuttleworth and C. M. Kielty, Mesenchymal stem cell migration is regulated by fibronectin through α5β1-integrin-mediated activation of PDGFR-β and potentiation of growth factor signals, *J. Cell Sci.*, 2011, **124**, 1288–1300.

18 F. Parnia, J. Yazdani and S. Maleki Dizaj, Applications of Mesenchymal Stem Cells in Sinus Lift Augmentation as a Dental Implant Technology, *Stem Cells Int.*, 2018, **2018**, 3080139.

19 Q. L. Ma, L. Fang, N. Jiang, L. Zhang, Y. Wang, Y. M. Zhang and L. H. Chen, Bone mesenchymal stem cell secretion of sRANKL/OPG/M-CSF in response to macrophage-mediated inflammatory response influences osteogenesis on nanostructured Ti surfaces, *Biomaterials*, 2018, **154**, 234–247.

20 L. C. Lopez, M. R. Belviso, R. Gristina, M. Nardulli, R. d'Agostino and P. Favia, Plasma-Treated Nitrogen-Containing Surfaces for Cell Adhesion: The Role of the Polymeric Substrate, *Plasma Processes Polym.*, 2007, **4**, S402–S405.

21 F. J. Harding, L. R. Clements, R. D. Short, H. Thissen and N. H. Voelcker, Assessing embryonic stem cell response to surface chemistry using plasma polymer gradients, *Acta Biomater.*, 2012, **8**, 1739–1748.

22 W. Zhang, J. Liu, H. Wang, Y. Xu, P. Wang, J. Ji and P. K. Chu, Enhanced cytocompatibility of silver-containing biointerface by constructing nitrogen functionalities, *Appl. Surf. Sci.*, 2015, **349**, 327–332.

23 W. Zhang, N. Liu, H. Shi, J. Liu, L. Shi, B. Zhang, H. Wang, J. Ji and P. K. Chu, Upregulation of BMSCs osteogenesis by positively-charged tertiary amines on polymeric implants via charge/iNOS signaling pathway, *Sci. Rep.*, 2015, **5**, 9369.

24 X. Li, N. Liu, Y. Wang, J. Liu, H. Shi, Z. Qu, T. Du, B. Guo and B. Gu, Brain and muscle aryl hydrocarbon receptor nuclear translocator-like protein-1 cooperates with glycogen synthase kinase-3beta to regulate osteogenesis of bone-marrow mesenchymal stem cells in type 2 diabetes, *Mol. Cell. Endocrinol.*, 2017, **440**, 93–105.

25 A. Hafezeqoran and R. Koodaryan, Effect of Zirconia Dental Implant Surfaces on Bone Integration: A Systematic Review and Meta-Analysis, *Biomed. Res. Int.*, 2017, **2017**, 9246721.

26 M. Ferraris, E. Verné, P. Appendino, C. Moisescu, A. Krajewski, A. Ravaglioli and A. Piancastelli, Coatings on zirconia for medical applications, *Biomaterials*, 2000, **21**, 765–773.

27 S. Cha and Y. S. Park, Plasma in dentistry, *Clin. Plasma Med.*, 2014, **2**, 4–10.

28 S. Mei, H. Wang, W. Wang, L. Tong, H. Pan, C. Ruan, Q. Ma, M. Liu, H. Yang, L. Zhang, Y. Cheng, Y. Zhang, L. Zhao and P. K. Chu, Antibacterial effects and biocompatibility of titanium surfaces with graded silver incorporation in titania nanotubes, *Biomaterials*, 2014, **35**, 4255–4265.

29 Y. Tian, H. Cao, Y. Qiao, F. Meng and X. Liu, Antibacterial activity and cytocompatibility of titanium oxide coating modified by iron ion implantation, *Acta Biomater.*, 2014, **10**, 4505–4517.

30 A. J. Wagner, D. H. Fairbrother and F. Reniers, A Comparison of PE Surfaces Modified by Plasma Generated Neutral Nitrogen Species and Nitrogen Ions, *Plasmas Polym.*, 2003, **8**, 119–134.

31 W. Zhang, H. Wang, A. Oyane, H. Tsurushima and P. K. Chu, Osteoblast differentiation and disinfection induced by nitrogen plasma-treated surfaces, *Bio-Med. Mater. Eng.*, 2011, **21**, 75–82.

32 J. Chevalier, L. Gremillard, A. V. Virkar and D. R. Clarke, The Tetragonal-Monoclinic Transformation in Zirconia: Lessons Learned and Future Trends, *J. Am. Ceram. Soc.*, 2009, **92**, 1901–1920.

33 I. A. Morozov, A. S. Mamaev, I. V. Osorgina, L. M. Lemkina, V. P. Korobov, A. Y. Belyaev, S. E. Porozova and M. G. Sherban, Structural-mechanical and antibacterial properties of a soft elastic polyurethane surface after plasma immersion N2(+) implantation, *Mater. Sci. Eng., C*, 2016, **62**, 242–248.

34 W. Zhang, Y. Luo, H. Wang, J. Jiang, S. Pu and P. K. Chu, Ag and Ag/N2 plasma modification of polyethylene for the enhancement of antibacterial properties and cell growth/proliferation, *Acta Biomater.*, 2008, **4**, 2028–2036.

35 Z. Gugala and S. Gogolewski, Attachment, growth, and activity of rat osteoblasts on polylactide membranes treated with various low-temperature radiofrequency plasmas, *J. Biomed. Mater. Res., Part A*, 2006, **76**, 288–299.

36 D. J. Gorth, S. Puckett, B. Ercan, T. J. Webster, M. Rahaman and B. S. Bal, Decreased bacteria activity on Si_3N_4 surfaces compared with PEEK or titanium, *Int. J. Nanomed.*, 2012, **7**, 4829–4840.

37 W. Zhang, J. Liu, H. Shi, K. Yang, P. Wang, G. Wang, N. Liu, H. Wang, J. Ji and P. K. Chu, Communication between nitric oxide synthase and positively-charged surface and bone formation promotion, *Colloids Surf., B*, 2016, **148**, 354–362.

38 D. Buser, R. K. Schenk, S. Steinemann, J. P. Fiorellini, C. H. Fox and H. Stich, Influence of surface characteristics on bone integration of titanium implants. A

histomorphometric study in miniature pigs, *J. Biomed. Mater. Res.*, 1991, **25**, 889–902.

39 A. Wennerberg, T. Albrektsson, B. Andersson and J. J. Krol, A histomorphometric and removal torque study of screw-shaped titanium implants with three different surface topographies, *Clin. Oral Implants Res.*, 1995, **6**, 24–30.

40 K. Gan, H. Liu, L. Jiang, X. Liu, X. Song, D. Niu, T. Chen and C. Liu, Bioactivity and antibacterial effect of nitrogen plasma immersion ion implantation on polyetheretherketone, *Dent. Mater.*, 2016, **32**, e263–e274.

41 A. Kondyurin, K. Lau, F. Tang, B. Akhavan, W. Chrzanowski, M. S. Lord, J. Rnjak-Kovacina and M. M. Bilek, Plasma Ion Implantation of Silk Biomaterials Enabling Direct Covalent Immobilization of Bioactive Agents for Enhanced Cellular Responses, *ACS Appl. Mater. Interfaces*, 2018, **10**, 17605–17616.

42 F. Y. Cao, J. X. Fan, Y. Long, X. Zeng and X. Z. Zhang, A smart fluorescence nanoprobe for the detection of cellular alkaline phosphatase activity and early osteogenic differentiation, *Nanomedicine*, 2016, **12**, 1313–1322.

43 S. Samavedi, A. R. Whittington and A. S. Goldstein, Calcium phosphate ceramics in bone tissue engineering: a review of properties and their influence on cell behavior, *Acta Biomater.*, 2013, **9**, 8037–8045.

44 P. Chatakun, R. Núñez-Toldrà, E. J. Díaz López, C. Gil-Recio, E. Martínez-Sarrà, F. Hernández-Alfaro, E. Ferrés-Padró, L. Giner-Tarrida and M. Atari, The effect of five proteins on stem cells used for osteoblast differentiation and proliferation: a current review of the literature, *Cell. Mol. Life Sci.*, 2014, **71**, 113–142.

45 M. Mizuno, R. Fujisawa and Y. Kuboki, Type I collagen-induced osteoblastic differentiation of bone-marrow cells mediated by collagen-alpha2beta1 integrin interaction, *J. Cell. Physiol.*, 2000, **184**, 207–213.

46 T. Komori, Runx2, a multifunctional transcription factor in skeletal development, *J. Cell. Biochem.*, 2002, **87**, 1–8.